

NLO QCD corrections to WW +jet production at hadron colliders

S. Dittmaier,¹ S. Kallweit,¹ and P. Uwer²

¹Max-Planck-Institut für Physik (Werner-Heisenberg-Institut), D-80805 München, Germany

²Institut für Theoretische Teilchenphysik, Universität Karlsruhe, D-76128 Karlsruhe, Germany

(Dated: October 31, 2018)

We report on the calculation of the next-to-leading order QCD corrections to the production of W -boson pairs in association with a hard jet at the Tevatron and the LHC, which is an important source of background for Higgs and new-physics searches. The corrections stabilize the leading-order prediction for the cross section considerably, in particular if a veto against the emission of a second hard jet is applied.

PACS numbers: 12.38.Bx, 13.85.-t, 14.70.Fm

INTRODUCTION

The search for new-physics particles—including the Standard Model Higgs boson—will be the primary task in high-energy physics after the start of the LHC that is planned for 2008. The extremely complicated hadron collider environment does not only require sufficiently precise predictions for new-physics signals, but also for many complicated background reactions that cannot entirely be measured from data. Among such background processes, several involve three, four, or even more particles in the final state, rendering the necessary next-to-leading-order (NLO) calculations in QCD very complicated. This problem led to the creation of an “experimenters’ wishlist for NLO calculations” [1, 2] that are still missing for successful LHC analyses. The process $pp \rightarrow W^+W^- + \text{jet} + X$ made it to the top of this list.

The process of WW +jet production is an important source for background to the production of a Higgs boson that subsequently decays into a W -boson pair, where additional jet activity might arise from the production or a hadronically decaying W boson. WW +jet production delivers also potential background to new-physics searches, such as supersymmetric particles, because of leptons and missing transverse momentum from the W decays. Last but not least the process is interesting in its own right, since W -pair production processes enable a direct precise analysis of the non-abelian gauge-boson self-interactions, and a large fraction of W pairs will show up with additional jet activity at the LHC.

In this letter we report on the first calculation of the process $pp \rightarrow W^+W^- + \text{jet} + X$ in NLO QCD.

DETAILS OF THE NLO CALCULATION

At leading order (LO), hadronic WW +jet production receives contributions from the partonic processes $q\bar{q} \rightarrow W^+W^-g$, $qg \rightarrow W^+W^-q$, and $\bar{q}g \rightarrow W^+W^-q$, where q stands for up- or down-type quarks. Note that the amplitudes for $q = u, d$ are not the same, even for vanishing light quark masses. All three chan-

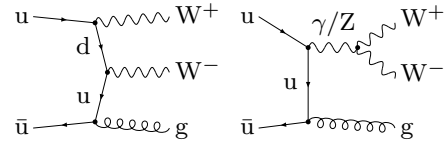


FIG. 1: Two representative LO diagrams for the partonic process $u\bar{u} \rightarrow W^+W^-g$.

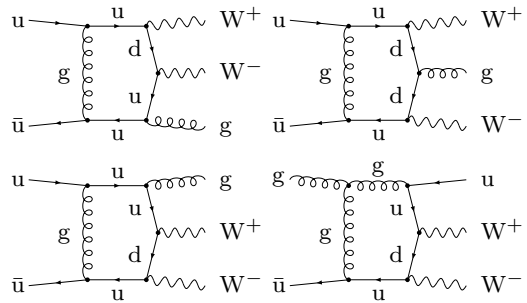


FIG. 2: Pentagon diagrams for the partonic process $u\bar{u} \rightarrow W^+W^-g$.

nels are related by crossing symmetry to the amplitude $0 \rightarrow W^+W^-q\bar{q}g$. Two representative LO diagrams for the process $u\bar{u} \rightarrow W^+W^-g$ are shown in Figure 1.

In order to prove the correctness of our results we have evaluated each ingredient twice using independent calculations based—as far as possible—on different methods, yielding results in mutual agreement.

Virtual corrections

The virtual corrections modify the partonic processes that are already present at LO. At NLO these corrections are induced by self-energy, vertex, box (4-point), and pentagon (5-point) corrections. For illustration the pentagon graphs, which are the most complicated diagrams, are shown in Figure 2 for a partonic channel. At one loop WW +jet production also serves as an off-shell continuation of the loop-induced process of Higgs+jet production with the Higgs boson decaying into a W -boson pair. In

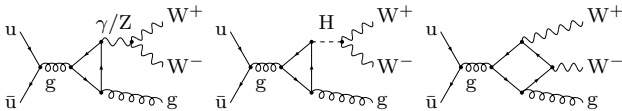


FIG. 3: Some diagrams with closed quark loops for the partonic process $u\bar{u} \rightarrow W^+W^-g$.

this subprocess the off-shell Higgs boson is coupled via a heavy-quark loop to two gluons; a sample graph for this mechanism is shown in Figure 3 together with some other typical graphs with a closed quark loop.

Version 1 of the virtual corrections is essentially obtained as for the related processes of $t\bar{t}H$ [3] and $t\bar{t}+\text{jet}$ [4] production. Feynman diagrams and amplitudes are generated with *FeynArts* 1.0 [5] and further processed with in-house *Mathematica* routines, which automatically create an output in *Fortran*. The IR (soft and collinear) singularities are treated in dimensional regularization and analytically separated from the finite remainder as described in Refs. [3, 6]. The pentagon tensor integrals are directly reduced to box integrals following Ref. [7]. This method does not introduce inverse Gram determinants in this step, thereby avoiding numerical instabilities in regions where these determinants become small. Box and lower-point integrals are reduced à la Passarino–Veltman [8] to scalar integrals, which are either calculated analytically or using the results of Refs. [9, 10, 11]. Sufficient numerical stability is already achieved in this way, but further improvements with the methods of Ref. [12] are in progress.

Version 2 of the evaluation of loop diagrams starts with the generation of diagrams and amplitudes via *FeynArts* 3.2 [13] which are then further manipulated with *FormCalc* 5.2 [14] and eventually automatically translated into *Fortran* code. The whole reduction of tensor to scalar integrals is done with the help of the *LoopTools* library [14], which also employs the method of Ref. [7] for the 5-point tensor integrals, Passarino–Veltman [8] reduction for the lower-point tensors, and the *FF* package [15, 16] for the evaluation of regular scalar integrals. The dimensionally regularized soft or collinear singular 3- and 4-point integrals had to be added to this library. To this end, the explicit results of Ref. [6] for the vertex and of Ref. [17] for the box integrals (with appropriate analytical continuations) are taken.

Real corrections

The matrix elements for the real corrections are given by $0 \rightarrow W^+W^-q\bar{q}gg$ and $0 \rightarrow W^+W^-q\bar{q}q'\bar{q}'$ with a large variety of flavour insertions for the light quarks q and q' . The partonic processes are obtained from these matrix elements by all possible crossings of quarks and gluons into the initial state. The evaluation of the real-

emission amplitudes is performed in two independent ways. Both evaluations employ (independent implementations of) the dipole subtraction formalism [18] for the extraction of IR singularities and for their combination with the virtual corrections.

Version 1 employs the Weyl–van-der-Waerden formalism (as described in Ref. [19]) for the calculation of the helicity amplitudes. The phase-space integration is performed by a multi-channel Monte Carlo integrator [20] with weight optimization [21] written in *C++*, which is constructed similar to *RacoonWW* [22, 23]. The results for cross sections with two resolved hard jets have been checked against results obtained with *Whizard* 1.50 [24] and *Sherpa* 1.0.8 [25]. Details on this part of the calculation can be found in Ref. [26]. In order to improve the integration, additional channels are included for the integration of the difference of the real-emission matrix elements and the subtraction terms.

Version 2 is based on scattering amplitudes calculated with *Madgraph* [27] generated code. The code has been modified to allow for a non-diagonal quark mixing matrix and the extraction of the required colour and spin structure. The latter enter the evaluation of the dipoles in the Catani–Seymour subtraction method. The evaluation of the individual dipoles was performed using a *C++* library developed during the calculation of the NLO corrections for $t\bar{t}+\text{jet}$ [4]. For the phase-space integration a simple mapping has been used where the phase space is generated from a sequential splitting.

NUMERICAL RESULTS

We consistently use the CTEQ6 [28, 29] set of parton distribution functions (PDFs), i.e. we take CTEQ6L1 PDFs with a 1-loop running α_s in LO and CTEQ6M PDFs with a 2-loop running α_s in NLO. We do not include bottom quarks in the initial or final states, because the bottom PDF is suppressed w.r.t. to the others; outgoing $b\bar{b}$ pairs add little to the cross section and can be experimentally further excluded by anti- b -tagging. Quark mixing between the first two generations is introduced via a Cabibbo angle $\theta_C = 0.227$. In the strong coupling constant the number of active flavours is $N_F = 5$, and the respective QCD parameters are $\Lambda_5^{LO} = 165 \text{ MeV}$ and $\Lambda_5^{\overline{\text{MS}}} = 226 \text{ MeV}$. The top-quark loop in the gluon self-energy is subtracted at zero momentum. The running of α_s is, thus, generated solely by the contributions of the light quark and gluon loops. The top-quark mass is $m_t = 174.3 \text{ GeV}$, the masses of all other quarks are neglected. The weak boson masses are $M_W = 80.425 \text{ GeV}$, $M_Z = 91.1876 \text{ GeV}$, and $M_H = 150 \text{ GeV}$. The weak mixing angle is set to its on-shell value, i.e. fixed by $c_w^2 = 1 - s_w^2 = M_W^2/M_Z^2$, and the electromagnetic coupling constant α is derived from Fermi's constant $G_\mu = 1.16637 \times 10^{-5} \text{ GeV}^{-2}$ according to $\alpha = \sqrt{2}G_\mu M_W^2 s_w^2/\pi$.

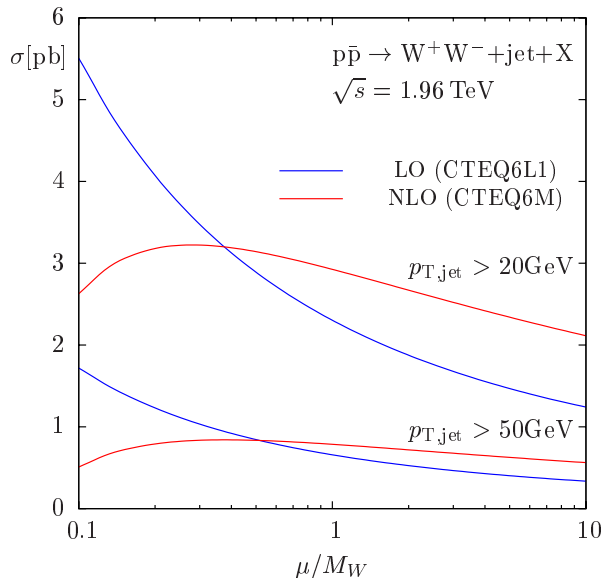


FIG. 4: Scale dependence of the LO and NLO cross sections for WW+jet production at the Tevatron, where the renormalization and factorization scales are set equal to μ .

We apply the jet algorithm of Ref. [30] with $R = 1$ for the definition of the tagged hard jet and restrict the transverse momentum of the hardest jet by $p_{T,\text{jet}} > p_{T,\text{jet,cut}}$. In contrast to the real corrections the LO prediction and the virtual corrections are not influenced by the jet algorithm. In our default setup, a possible second hard jet (originating from the real corrections) does not affect the event selection, but alternatively we also consider mere WW+jet events with “no 2nd separable jet” where only the first hard jet is allowed to pass the $p_{T,\text{jet}}$ cut but not the second.

Figures 4 and 5 show the scale dependence of the integrated LO and NLO cross sections at the Tevatron and the LHC, respectively. The renormalization and factorization scales are identified here ($\mu = \mu_{\text{ren}} = \mu_{\text{fact}}$), and the variation ranges from $\mu = 0.1 M_W$ to $\mu = 10 M_W$.

The dependence is rather large in LO, illustrating the well-known fact that the LO predictions can only provide a rough estimate. At the Tevatron the $q\bar{q}$ channels dominate the total $p\bar{p}$ cross section by about 90%, followed by the qg and $\bar{q}g$ channels with about 5% each. Scaling the renormalization and factorization scales simultaneously by a factor of 4 (10) changes the cross section by about 70% (100%). At the LHC, the qg channels comprise about 56%, followed by $q\bar{q}$ with about 28%. Surprisingly the scale dependence is much smaller than at the Tevatron: varying the scales simultaneously by a factor of 4 (10) changes the cross section by about 25% (50%).

At the Tevatron (Figure 4), the NLO corrections significantly reduce the scale dependence for $p_{T,\text{jet}} > 20$ GeV and 50 GeV. We observe that around $\mu \approx M_W$ the NLO corrections are of moderate size for the chosen setup. At the LHC (Figure 5), only a modest reduction of the scale

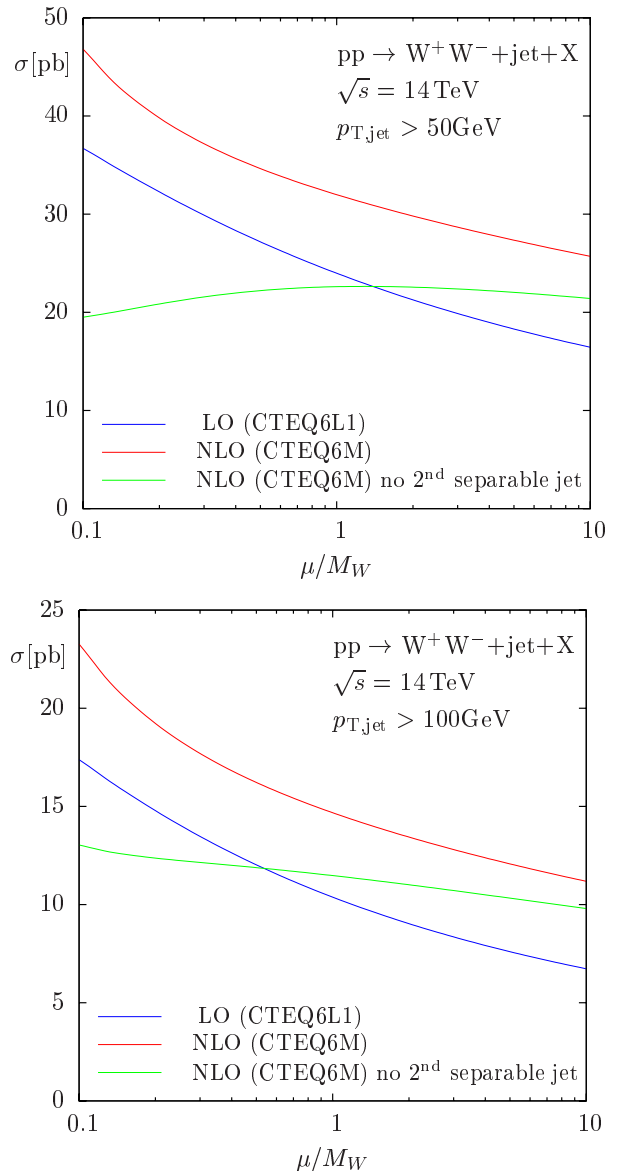


FIG. 5: Scale dependence of the LO and NLO cross sections for WW+jet production at the LHC, where the renormalization and factorization scales are set equal to μ .

dependence is observed in the transition from LO to NLO if W pairs in association with two hard jets are taken into account. This large residual scale dependence in NLO, which is mainly due to qg -scattering channels, can be significantly suppressed upon applying the veto of having “no 2nd separable jet”. The contribution of the genuine WW+2jets events, which represents the difference between the two NLO curves in the plots of Figure 5, is also reduced if the cut on $p_{T,\text{jet}}$ is increased from 50 GeV to 100 GeV. The relevance of a jet veto in order to suppress the scale dependence at NLO was also realized [31] for genuine W-pair production at hadron colliders.

Finally, we show the integrated LO and NLO cross sections as functions of $p_{T,\text{jet,cut}}$ in Figure 6. The widths of

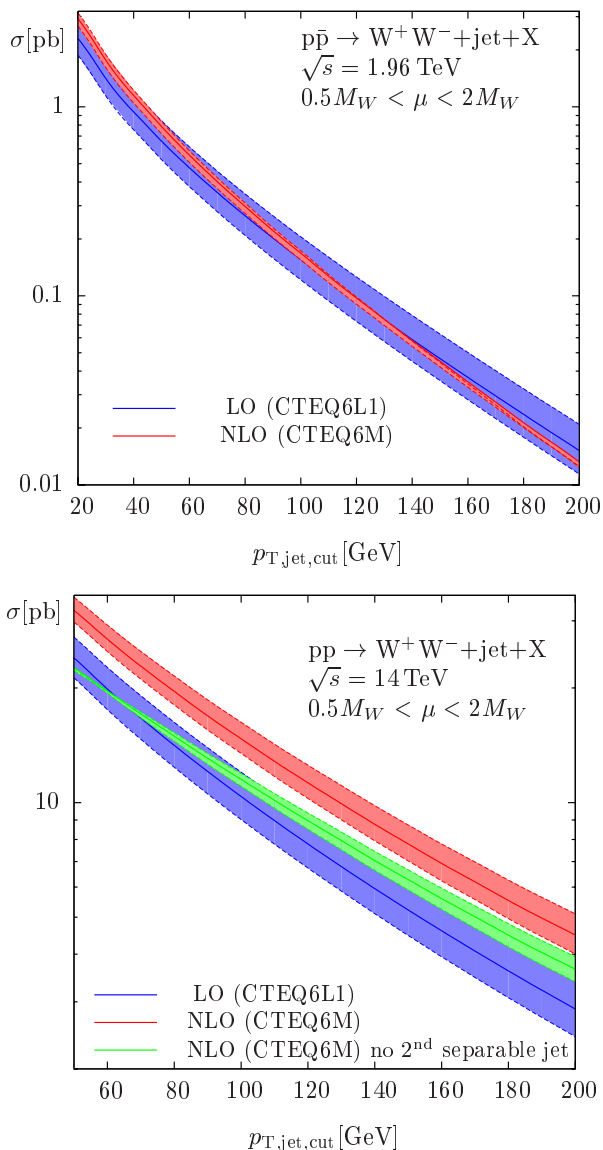


FIG. 6: LO and NLO cross sections for $WW+\text{jet}$ production at the Tevatron and LHC as function of $p_{T,\text{jet,cut}}$.

the bands, which correspond to scale variations within $M_W/2 < \mu < 2M_W$, reflect the behaviour discussed above for fixed values of $p_{T,\text{jet,cut}}$. For Tevatron the reduction of the scale uncertainty is considerable, for the LHC it is only mild unless $WW+2\text{jets}$ events are vetoed.

Acknowledgment: P.U. is supported as Heisenberg Fellow of the Deutsche Forschungsgemeinschaft DFG. S.D. and P.U. thank the Galileo Galilei Institute for Theoretical Physics in Florence for the hospitality and the INFN for partial support during the completion of this work. This work is supported in part by the European Community's Marie-Curie Research Training Network HEP-TOOLS under contract MRTN-CT-2006-035505 and by the DFG Sonderforschungsbereich/Transregio 9 "Computergestützte Theoretische Teilchenphysik" SFB/TR9.

- [1] C. Buttar et al. (2006), hep-ph/0604120.
- [2] J. M. Campbell, J. W. Huston, and W. J. Stirling, Rept. Prog. Phys. **70**, 89 (2007), hep-ph/0611148.
- [3] W. Beenakker et al., Nucl. Phys. **B653**, 151 (2003), hep-ph/0211352.
- [4] S. Dittmaier, P. Uwer, and S. Weinzierl, Phys. Rev. Lett. **98**, 262002 (2007), hep-ph/0703120.
- [5] J. Küblbeck, M. Böhm, and A. Denner, Comput. Phys. Commun. **60**, 165 (1990).
- [6] S. Dittmaier, Nucl. Phys. **B675**, 447 (2003), hep-ph/0308246.
- [7] A. Denner and S. Dittmaier, Nucl. Phys. **B658**, 175 (2003), hep-ph/0212259.
- [8] G. Passarino and M. J. G. Veltman, Nucl. Phys. **B160**, 151 (1979).
- [9] G. 't Hooft and M. J. G. Veltman, Nucl. Phys. **B153**, 365 (1979).
- [10] W. Beenakker and A. Denner, Nucl. Phys. **B338**, 349 (1990).
- [11] A. Denner, U. Nierste, and R. Scharf, Nucl. Phys. **B367**, 637 (1991).
- [12] A. Denner and S. Dittmaier, Nucl. Phys. **B734**, 62 (2006), hep-ph/0509141.
- [13] T. Hahn, Comput. Phys. Commun. **140**, 418 (2001), hep-ph/0012260.
- [14] T. Hahn and M. Perez-Victoria, Comput. Phys. Commun. **118**, 153 (1999), hep-ph/9807565.
- [15] G. J. van Oldenborgh and J. A. M. Vermaseren, Z. Phys. **C46**, 425 (1990).
- [16] G. J. van Oldenborgh, Comput. Phys. Commun. **66**, 1 (1991).
- [17] Z. Bern, L. J. Dixon, and D. A. Kosower, Nucl. Phys. **B412**, 751 (1994), hep-ph/9306240.
- [18] S. Catani and M. H. Seymour, Nucl. Phys. **B485**, 291 (1997), hep-ph/9605323.
- [19] S. Dittmaier, Phys. Rev. **D59**, 016007 (1999), hep-ph/9805445.
- [20] F. A. Berends, R. Pittau, and R. Kleiss, Nucl. Phys. **B424**, 308 (1994), hep-ph/9404313.
- [21] R. Kleiss and R. Pittau, Comput. Phys. Commun. **83**, 141 (1994), hep-ph/9405257.
- [22] A. Denner, S. Dittmaier, M. Roth, and D. Wackerroth, Nucl. Phys. **B560**, 33 (1999), hep-ph/9904472.
- [23] M. Roth, PhD thesis, ETH Zurich No. 13363 (1999), hep-ph/0008033.
- [24] W. Kilian, WHIZARD manual (2001), IC-TOOL-2001-039.
- [25] T. Gleisberg et al., JHEP **02**, 056 (2004), hep-ph/0311263.
- [26] S. Kallweit, diploma thesis (in German), LMU Munich (2006).
- [27] T. Stelzer and W. F. Long, Comput. Phys. Commun. **81**, 357 (1994), hep-ph/9401258.
- [28] J. Pumplin et al., JHEP **07**, 012 (2002), hep-ph/0201195.
- [29] D. Stump et al., JHEP **10**, 046 (2003), hep-ph/0303013.
- [30] S. D. Ellis and D. E. Soper, Phys. Rev. **D48**, 3160 (1993), hep-ph/9305266.
- [31] L. J. Dixon, Z. Kunszt, and A. Signer, Phys. Rev. **D60**, 114037 (1999), hep-ph/9907305.